Methods of density estimation for pedestrians moving without a spatial boundary

 $\begin{array}{c} \text{Pratik Mullick}^{1[0000-0003-0133-0354]}, \text{ C\'ecile} \\ \text{Appert-Rolland}^{2[0000-0002-0985-6230]}, \text{ William H. Warren}^{3[0000-0003-4843-2315]}, \\ \text{and Julien Pettr\'e}^{1[0000-0003-1812-1436]} \end{array}$

 Univ Rennes, INRIA, CNRS, IRISA, Rennes, France
 Université Paris-Saclay, CNRS/IN2P3, IJCLab, Orsay, France
 Department of Cognitive, Linguistic and Psychological Sciences, Brown University, Providence, Rhode Island, USA

Abstract. For a crowd without any spatial boundaries, the methods of density estimation is a wide area of research. In the existing literature, Voronoi-cell based density estimation is widely used. We focus on the typical situation of crossing flows of pedestrians for which we use an experimental data set. We explore several other methods of density estimation for crossing flows in an open space. The density estimation methods consisted of both Lagrangian and Eulerian approaches, as well as the Voronoi-cell based method. To find the correct set of parameters to define density by a method, we compare the estimations with that obtained by Voronoi-cell based method. We do this by minimizing ε_i , where.

$$\varepsilon_i = \sqrt{\frac{1}{N} \sum (\rho_{\rm vc} - \rho_i)^2}.$$

N denotes the number of pedestrians, $\rho_{\rm vc}$ is the density estimated by Voronoi method and ρ_i is the density obtained by the method for which we intend to find the correct set of parameters. We also use detrended fluctuation analysis (DFA) to identify the method that provides the measurement with least fluctuations.

Keywords: Crowd motion \cdot Density estimation \cdot Detrended fluctuation analysis.

1 Introduction

In the context of self-organizing behaviour of human crowd motion, methods of density estimation are an important topic of research. Existing literature consists of a number of methods, however depending on the crowd situation a debate for the 'best' method has not yet been resolved. Most of the research have been focused on situations where the moving crowd is constrained within a physical boundary. For such cases, density estimation using Voronoi tesselation [3,8,6,9,2] and a grid-based measure called XT method [4,3] have been reported to work well. However, there lacks a well defined method of density estimation for crowd scenarios in an unbounded space.

From the point of view of crowd management, understanding the fundamental relation between crowd density and speed, i.e. fundamental diagram (FD), is extremely useful. Also for simulation based findings, FD acts as an essential tool to evaluate the capacity of simulations to predict realistic pedestrian flow. Thus, to construct a realistic FD, an effective method of density estimation is required.

For our research, we consider crossing flows of pedestrians without any spatial constraints, where two groups of people follow only visual instructions to cross each other at specified values of the crossing angle α . In the context of crossing flows, most of the previous investigations have been concentrated on $\alpha=90^\circ$ & 180°. We performed experimental trials for a wide range of values of α with the goal to study crossing angle dependent properties. Currently, we want to investigate how the density-speed relationship for crossing flows is affected by the value of crossing angle. Along with the previously existing methods to evaluate pedestrian density, we also introduce a new method in this contribution and present a comparative analysis across various methods.

Experimental details: The data for crossing flows of pedestrians used for this research were obtained by experiments [1,5] using live participants on campus of University of Rennes, France. Two different sets of volunteered participants (36 on Day 1, 38 on Day 2) were roughly divided into two groups (18 or 19 per group) and were instructed to walk through each other at seven different crossing angles (0° to 180°, at 30° intervals). During each trial we recorded the head trajectory of each pedestrian as a time series at a frequency of 120 Hz using an infrared camera system. In Fig. 1 we show the traces of all the pedestrians for a typical trial using filtered trajectories.

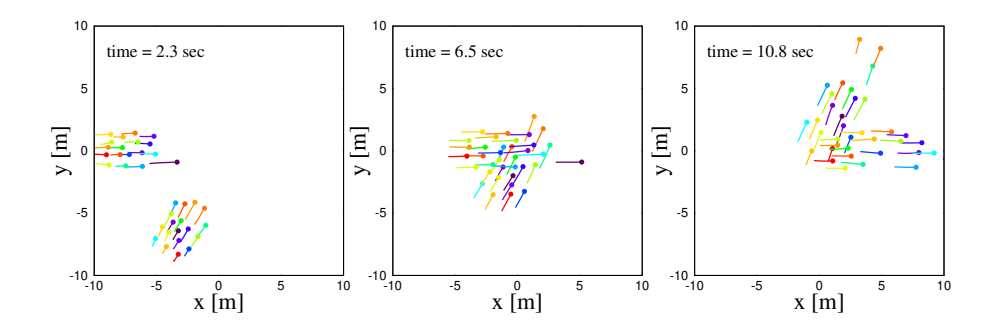


Fig. 1. Figure shows traces of all the pedestrians involved in a typical trial whose crossing angle is expected to be 60° . The dots represent the pedestrians and the tails behind each dot are the distances travelled by the pedestrian in previous 1.25 sec.

2 Methods for estimating pedestrian density ρ

2.1 Grid-based classical method

The classical method to estimate the density of pedestrians follows an Eulerian approach. We divide the entire tracking region into square-shaped grids. For d_g to be the length of these grids, the classical density $\rho_{\rm g}$ is given by $\rho_{\rm g} = n/{d_g}^2$, where n is the number of pedestrians that are located inside the grid. The density estimated for each grid is associated to all the pedestrians that are within it. In Fig. 2(a) we show the time-sequence of classical density $\rho_{\rm g}$ for a typical pedestrian for several values of the grid size d_g . For smaller grid sizes, the density values keep switching between only a few levels - which signifies the discrete nature of $\rho_{\rm g}$.

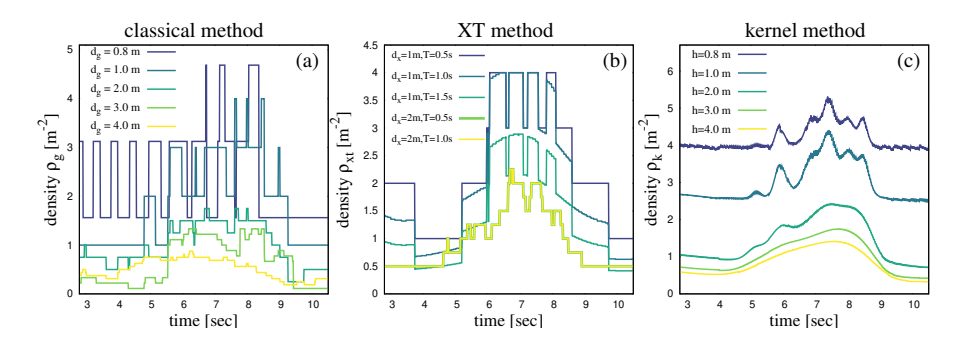


Fig. 2. Variation of several definitions of density for a typical pedestrian as a function of time. (a) Time sequences of $\rho_{\rm g}$ for various values of grid size d_g . (b) Time sequences of $\rho_{\rm xt}$ for various values of cell size d_x and time period T. (c) Time sequences of $\rho_{\rm k}$ for various values of bandwidth h.

2.2 XT method

The XT method was originally proposed by Edie [4]. Later, this method was modified [3], which we have used to compute the pedestrian density. A square-shaped cell c of length d_x is considered at whose center a pedestrian p is located at time t. There could be other pedestrians as well within this cell at time t. The density $\rho_{\rm xt}(c,t)$ estimated for cell c at time t is associated to the pedestrian p and is given by

$$\rho_{\rm xt}(c,t) = \frac{\sum (T_{\rm end} - T_{\rm begin})}{{d_x}^2 \times T},\tag{1}$$

where the summation is performed over all the pedestrians placed inside the cell c at time t. $T_{\rm begin}$ denotes the maximum of the time when the pedestrian enters the cell c and the lower time boundary t-0.5T, and $T_{\rm end}$ denotes the minimum of the time when the pedestrian exits the cell c and the upper time boundary

4

t+0.5T. The time period T restricts the time window of the pedestrians during which they are accounted for the computation. Previous investigations lack any rigorous argument for the choice of d_x and T that would produce a physically realistic estimate of density experience by each pedestrian. Fig. 2(b) shows the time sequence of the density ρ_{xt} for a typical pedestrian for several values of d_x and T. The estimate of the density is seen to decrease with the increase of both d_x and T, as indicated by Eq. (1). The overall nature of ρ_{xt} shows less smoothness which reflects the discrete nature of its definition.

2.3 Kernel method

For density estimation of pedestrians on a 2D surface we introduce a non-parametric Lagrangian approach by using the kernel density estimator (KDE). In the context of crowd density estimation, this method has never been used to the best of our knowledge. KDE basically evaluates the probability density function using kernels at each pedestrian position, from which we calculate the physical density field of the entire tracking region by using appropriate normalisation. For $\mathbf{X}_1, \mathbf{X}_2, \mathbf{X}_3...\mathbf{X}_N$ to be the collection of 2D coordinates for N agents, the density function ρ_k estimated by the kernel density method at the spatial position \mathbf{X} is given by,

$$\rho_{\mathbf{k}}^{\mathbf{h}}(\mathbf{X}) = \sum_{i=1}^{N} K_{\mathbf{h}}(\mathbf{X} - \mathbf{X}_i), \tag{2}$$

where \mathbf{h} is the bandwidth dictating the smoothness of the density estimation. Among the several choices of the kernel function K, we use the bi-variate Gaussian distribution function $K_{\mathbf{h}} = \frac{1}{2\pi} |\mathbf{h}|^{-\frac{1}{2}} e^{-\frac{1}{2} \mathbf{X}^T \mathbf{h}^{-1} \mathbf{X}}$. \mathbf{h} is supposed to be a 2×2 matrix in 2D that would contain a vector of bandwidths for the two dimensions to control the amount and orientation of smoothness. However we use a scalar value as the bandwidth h that was taken to apply in both directions. From the estimated function $\rho_{\mathbf{k}}(\mathbf{X})$, we finally estimate the density at each of the pedestrian positions and associate the density to the corresponding pedestrian. Fig. $2(\mathbf{c})$ shows the time sequences of the density $\rho_{\mathbf{k}}$ for a typical pedestrian for several values of the bandwidth h.

2.4 Voronoi method

Density estimation of human crowd using Voronoi cells has been a very popular method [3,8,6,2,9]. We construct the Voronoi diagram of the pedestrians at every instant of the trial. To deal with the agents located near the edges of the groups we used the modified convex hull of their positions as the bounding contour - a method previously used in [6]. The modification on the actual convex hull takes care of the angular adjustments for the agents located 'on' the convex hull and the agents whose Voronoi cell extend beyond the convex hull. In Figure 3, we show the Voronoi cells of the pedestrians bounded by their modified convex hull.

For an agent with $A_{\rm vc}$ as the area its Voronoi cell within the modified convex hull, the density $\rho_{\rm vc}$ is given by

$$\rho_{\rm vc} = \frac{1}{A_{\rm vc}}.\tag{3}$$

Figure 3 also shows the density fields for each of the pedestrians estimated using Eq. (3). In Figure 4 the variation of ρ_{vc} as a function of time has been plotted for a typical pedestrian.

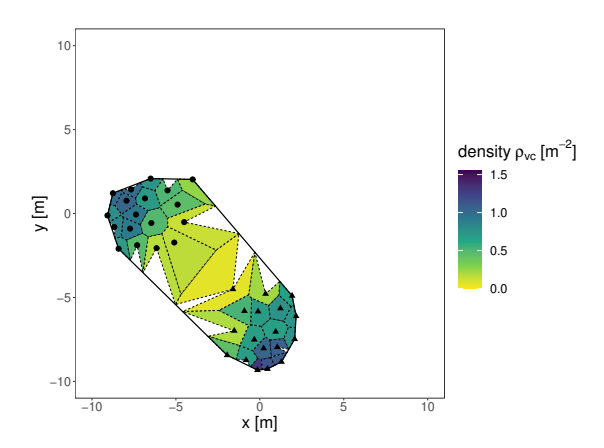


Fig. 3. Voronoi cells of the pedestrians bounded by their modified convex hull (dashed black line), for a typical trial of $\alpha=90^{\circ}$. The solid black line denotes the actual convex hull. The dots and triangles indicate the pedestrians from two groups, which move along the x-axis and y-axis respectively. The color bar indicates the density experienced by each pedestrian.

3 Optimising parameters: comparison with Voronoi method

Density estimations using the classical method, XT method and kernel method depends on the parameters which were key to their definitions. So the density values depend on the choice of these defining parameters. However the density estimation using Voronoi method does not require any such parameter except for the geometrical shape to clip the construction. For the estimations $\rho_{\rm g}$, $\rho_{\rm xt}$ and $\rho_{\rm k}$ to be comparable with $\rho_{\rm vc}$, i.e., to produce a realistic estimate, we define a numerical strategy to choose d_g for $\rho_{\rm g}$, (d_x,T) for $\rho_{\rm xt}$ and h for $\rho_{\rm k}$. For N pedestrians in a trial, we compute the quantity ε ,

$$\varepsilon_i = \sqrt{\frac{1}{N} \sum_{N} (\rho_{vc} - \rho_i)^2}$$
, where $i = g$, xt or k, (4)

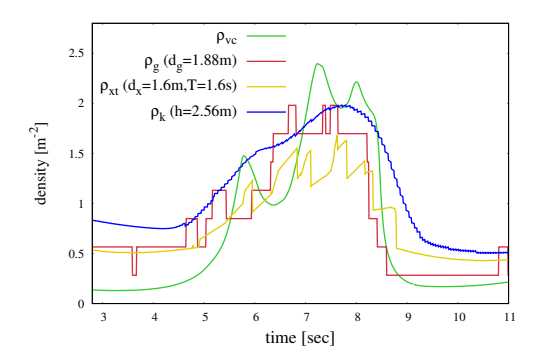


Fig. 4. Time sequences of density obtained by various methods for the pedestrian that was considered in Fig. 2. The parameters used to estimate $\rho_{\rm g}$, $\rho_{\rm xt}$ and $\rho_{\rm k}$ were optimised using Eq. 4.

as a time sequence with an interval of 1 sec and then compute the time-average. Finally, we choose the value of d_g , (d_x, T) or h which minimises the average value of ε over 7 randomly chosen trials (one per each crossing angle). Our findings from the optimization procedure are summarized in Table 1.

Table 1. Optimized parameters obtained by using Eq. 4.

Method	Quantity minimised	Obtained parameters
Classical	$arepsilon_{ m g}$	$d_g = 1.88 \text{m}$
XT	$arepsilon_{ ext{xt}}$	$d_x = 1.6 \text{m}, T = 1.6 \text{ sec}$
Kernel	$arepsilon_{ m k}$	h = 2.56 m

The variation of the quantities ε for each method as a function of their defining parameters are shown in Figs. 5(a), 5(b) and 5(c). The corresponding density fields obtained using the optimised parameters for all the pedestrians from a typical trial (as in Fig. 3) are shown in Figs. 5(d), 5(e) and 5(f). In Fig. 4 we also show the time sequence of the densities estimated using the optimised parameters for the typical pedestrian considered in Fig. 2.

4 Discussion and Conclusion

In this contribution we analyse four methods to estimate the density ρ of pedestrians moving without any spatial constraints. The classical method and the XT method provide a discrete nature of density - a consequence of using square shaped cells in both the cases. On the other hand, the densities obtained by the Voronoi method and the kernel method appears to be relatively smooth (Fig. 4).

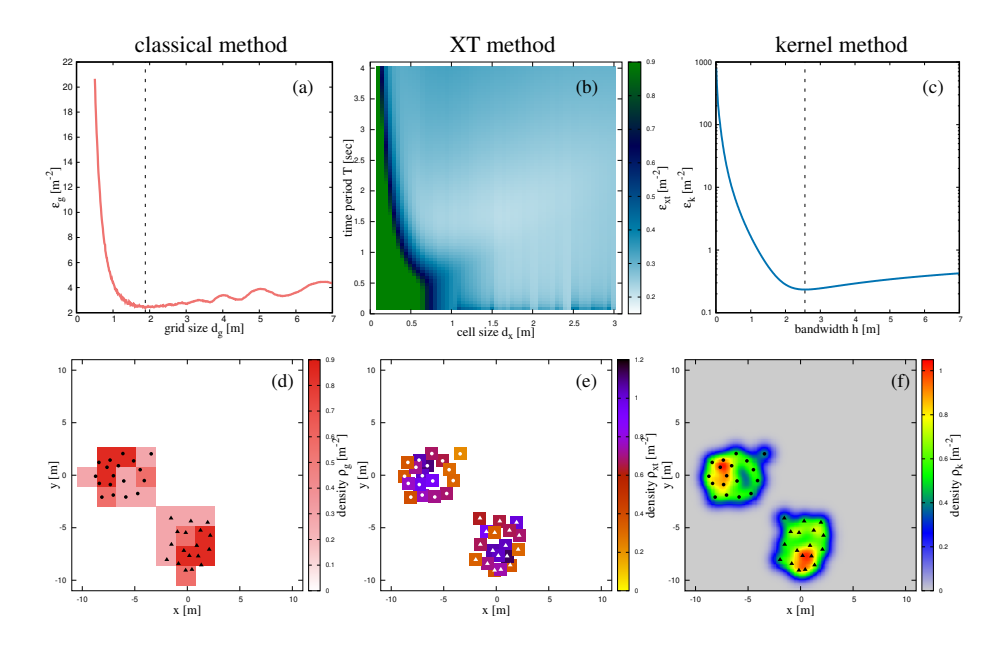


Fig. 5. Optimisation of the parameters defining various methods of density estimation and the density fields corresponding to the optimised parameters. (a) Variation of $\varepsilon_{\rm g}$ with grid size d_g for grid-based classical method. The minima occurs at $d_g=1.88{\rm m}$ and the corresponding density field is shown in (d). (b) Variation of $\varepsilon_{\rm xt}$ with cell size d_x and time period T for XT method. The minima occurs at $d_x=1.6{\rm m}$, T=1.6 sec and the corresponding density field is shown in (e). (c) Variation of $\varepsilon_{\rm k}$ with bandwidth h for kernel method. The minima occurs at h=2.56 and the corresponding density field is shown in (f). The trial for which the density fields are shown has $\alpha=90^{\circ}$ and is the same one shown in Fig. 3.

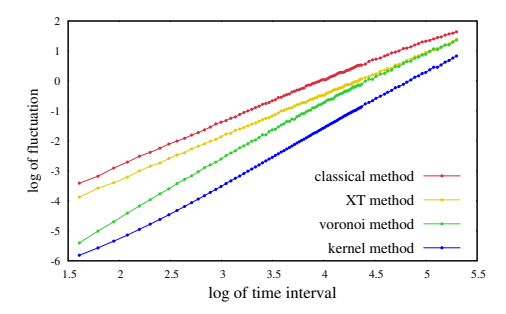


Fig. 6. Plot of $\log[F(t_n)]$ as a function of $\log(t_n)$ to perform detrended fluctuation analysis. The kernel method, staying lowest in the plot, indicates the method with least fluctuations.

We performed detrended fluctuation analysis (DFA) [7] to numerically conclude which method provides the 'smoothest' estimate, i.e., with least fluctua-

tions. DFA provides a categorical method to evaluate the degree of fluctuation at each time scale in a time-series. For each density method, we calculate the log of fluctuations $\log[F(t_n)]$ as a function of the log of time window $\log[t_n]$ for all the agents and compute the mean. We compute the mean DFA curve by taking average over 7 randomly chosen trials (one per each crossing angle) and are shown in Fig. 6. The results are as anticipated. The higher curves in the plot, i.e., the ones for classical method and XT method, indicate the methods with more fluctuations. Voronoi method and kernel method, staying low in the DFA plot, signifies the methods with lower fluctuations.

Furthermore, we use one-way ANOVA to statistically compare the y-positions of the mean curve for each method and found the results to be statistically significant, F(3,396), $p < 10^{-6}$, $\eta^2 = 0.164$. Therefore, we can conclude that the kernel method provides an estimate with the least fluctuations, as is also evident from Fig. 6. In our following research, we are going to use these density estimations to construct crossing angle dependent fundamental diagrams for crossing flows of crowds.

References

- Appert-Rolland, C., Pettré, J., Olivier, A.H., Warren, W., Duigo-Majumdar, A., et. all, E.P.: Experimental study of collective pedestrian dynamics. Collective Dynamics 5, 1–8 (2020). https://doi.org/ISSN: 2366–8539. https://doi.org/10.17815/CD.2020.109
- Cao, S., Seyfried, A., Zhang, J., Holl, S., Song, W.: Fundamental diagrams for multidirectional pedestrian flows. Journal of Statistical Mechanics: Theory and Experiment 2017(3), 033404 (mar 2017). https://doi.org/10.1088/1742-5468/aa620d
- 3. Duives, D.C., Daamen, W., Hoogendoorn, S.P.: Quantification of the level of crowdedness for pedestrian movements. Physica A: Statistical Mechanics and its Applications 427, 162–180 (2015). https://doi.org/10.1016/j.physa.2014.11.054
- 4. Edie, L.C.: Discussion of traffic stream measurements and definitions. Proceedings of the Second International Symposium on the Theory of Traffic Flow, London pp. 139–154 (1963)
- Mullick, P., Fontaine, S., Appert-Rolland, C., Olivier, A.H., Warren, W.H., Pettré, J.: Analysis of emergent patterns in crossing flows of pedestrians reveals an invariant of 'stripe' formation in human data. PLoS Comput Biol 18(6), e1010210 (2022). https://doi.org/https://doi.org/10.1371/journal.pcbi.1010210
- Nicolas, A., Kuperman, M., Ibañez, S., Bouzat, S., Appert-Rolland, C.: Mechanical response of dense pedestrian crowds to the crossing of intruders. Scientific Reports 9, 105 (2019). https://doi.org/10.1038/s41598-018-36711-7
- Peng, C.K., Buldyrev, S.V., Havlin, S., Simons, M., Stanley, H.E., Goldberger, A.L.: Mosaic organization of dna nucleotides. Phys. Rev. E 49, 1685–1689 (Feb 1994). https://doi.org/10.1103/PhysRevE.49.1685
- 8. Steffen, В., A.: for pedestrian Seyfried, Methods measuring density, flow, speed and direction with minimal scatter. Physica A: Sta-Mechanics and its Applications **389**(9), 1902 - 1910(2010).https://doi.org/https://doi.org/10.1016/j.physa.2009.12.015
- 9. Zhang, J., Klingsch, W., Rupprecht, T., Schadschneider, A., Seyfried, A.: Empirical study of turning and merging of pedestrian streams in t-junction (2011). https://doi.org/10.48550/ARXIV.1112.5299